Tri Dasa Mega Vol. 24 No. 2 (2022) 59–66

Jurnal Teknologi Reaktor Nuklir

Tri Dasa Mega

Journal homepage: jurnal.batan.go.id/index.php/tridam

Analysis of the RSG-GAS PPF Value Dependence on the Fuel Burnup

Lily Suparlina[1*], Purwadi Purwadi[2], Nabeshima Kunihiko[3]

[1]Research Center for Nuclear Reactor Technology, ORTN, BRIN, Kawasan Puspiptek Building No. 80, Tangerang Selatan 15310, Banten, Indonesia.
[2]Center for Multipurpose Reactor, ORTN, BRIN, Kawasan Puspiptek Building no. 30 Tangerang Selatan 15310, Banten, Indonesia.
3Nuclear Material Management Section, 4002 Narita-Cho, O-arai-machi, Higashi-Ibarakigun, Ibaraki 311-1393, Japan Atomic Energy Agency (JAEA), Japan.

ARTICLE INFO

Article history:

Received: 20 April 2022
Received in revised form: 4 June 2022
Accepted: 14 June 2022

Keywords:

RSG-GAS reactor
Reactor operation
Equilibrium core
BATAN-3DIFF
PPF value

A B S T R A C T

The RSG-GAS reactor has been operated in a safe and reliable manner for about 35 years since it commenced its operation in 1987 to serve radioisotopes production, NAA, neutron beam experiments, material irradiation, and reactor physics experimental activities as well as training purposes. Power peaking factor (PPF) has a strong relation to operation safety as well as service availability. Its value is necessary to determine by calculation since it is impossible to determine it experimentally in the core. This paper is intended to analyze the PPF values of the RSG-GAS reactor core as a function of burnup. The analysis was done using WIMSD-5B/BATAN-3DIFF computer codes. The result shows that the PPF values are significantly different for each burnup or energy in MWD. The values of axial and radial PPF are still under the safety limit and the BATAN-3DIFF code satisfyingly determines the PPF values of the RSG-GAS reactor core and supports the safety of reactor operation.

1. INTRODUCTION

Research reactors are essential tools for nuclear energy development. Irradiation of materials, components, and developing power fuel elements carried out in research reactors must safely meet the needs of industry and utilities [1]. The core of a research reactor contains fuel assemblies, moderators, reflectors, reactivity control devices (neutron poisons), and experimental apparatus. In many cases, these components are modular and are placed in prescribed locations on a grid plate to achieve an operational core to meet the needs of the current experimental programs while fulfilling the requirements of the Operating Limits and Conditions (OLCs). Research reactors are generally regulated by control rods (neutron absorbers). Control rods are an important component for maintaining the desired state of fission reactions within a nuclear reactor. They constitute a real-time control of the fission process, which is crucial for both keeping the fission chain reaction active and preventing it from accelerating beyond control. The state of a fission chain reaction can be concisely summarized by the effective multiplication factor, k, which indicates the change in the total number of fission events during successive generations of the chain reaction [2].

In the case of material irradiation of specific fuel tests, the total core excess reactivity, reactivity worth of control rods, shutdown margins, power density distribution, maximum linear power of the test sample, and power peaking factor (PPF) must all be estimated and verified in accordance with the OLCs of the reactor. Advanced irradiation and tests

[*] Corresponding author. Tel./Fax.: 021-7560912/021-7560913
E-mail: lilyrsg@batan.go.id
DOI: 10.17146/tdm.2022.24.2.6616

are typically performed at multipurpose research reactors, which have the flexibility to adjust sample power levels, sample average temperatures (in experimental devices), and the neutron flux spectrum and densities at the fuel samples locations through adjustment of the neutron absorbers, core design, reflector layout, or the experimental device layout. To determine core operating strategies that would permit maximum operating flexibility for reactor utilization while remaining within the OLCs, validated methods and codes should be utilized to determine core parameters. In this paper, three-dimensional, four-group diffusion calculations are verified according to the RSG-GAS MTR reactor [8, 9]. The macroscopic cell and core calculations are performed using the well-known reactor codes WIMSD-5B [10] using nuclear data ENDFBVII.1 and Batan-3DIFF [11] respectively. The reactivity worth effect of control rod movements and their shadow effect on the power distribution must be in accordance with the OLCs regarding a sufficient shutdown margin. In this research, a sensitivity analysis of the use of different absorber materials on the main safety parameters is conducted. The related safety quantities and parameters are as follows: core excess reactivity, shutdown margin, total reactivity worth of control rods, thermal neutron flux, power distribution, and PPF. Analysis of the effect of different burnup levels on the value of PPF at the RSG-GAS reactor is the concern of this calculation [12, 13].

The purpose of this research is to understand whether the PPF values change as a function of burnup or energy in MWD. The analysis is done using the WIMSD/BATAN-3DIFF codes. The analyzed parameters are core excess reactivity, shut down reactivity, shut down margin reactivity, and PPF. These parameters are critical for the safety of the reactor operation.

2. BRIEF DESCRIPTION OF RSG-GAS

RSG-GAS research reactor [14, 15] is a pool-type research reactor cooled and moderated by light water, which uses beryllium (as depicted in Figure 1) as a reflector material. It can operate at a nominal power of 30 MW. It uses MTR fuel elements with low and high-enriched uranium. In this study, only the low enriched uranium (LEU) fuel is considered. The defined reference core (Figure 1) has a 10×10 grid filled with 40 Standard Fuel Elements (SFE), 8 Control Fuel Elements (CFE), and a central irradiation position composed of (H_2O+Al). The fuel elements consist of 21 fuel plates of SFE type and 15 fuel plates of CFE type. Two separate regions in CFE are dedicated to fork-type absorber blades. Figures 2 and 3 show the SFE and CFE, respectively. The reactor core is placed inside a light water pool, cooled by downward forced convection, and reflected by two opposite rows of beryllium. Table 1 summarizes the main parameters of the reactor.

Table 1. Neutronic Design Parameters [15]

Core Characteristics	Values
Amount of fuel elements	40
Amount of control elements	8
Amount of absorbers	8
Cycle length (at full power), MWD	750
The average fuel burnup, BOC, % loss of ^{235}U	25.60
Average burnup at EOC,% loss of ^{235}U	32.53
Average discharged fuel burnup, % loss of ^{235}U	55.50
Max. burnup,% loss of ^{235}U	59.91
Excess reactivity at BOC, %	7.69
Reactivity for experiments,%	3.00
Total reactivity value of 8 control rods,%	-14.07
Shut-down reactivity margin, %	-2.35
Stuck rod condition, %	≥ - 0.5
Coefficient of fuel temperature, %Δk/k	-1.92×10^{-5}
Coefficient of moderator temperature, %Δk/k	-7.60×10^{-5}
Coefficient of moderator void, %Δk/k	-1.36×10^{-3}
Delayed neutron fraction	0.007186
Lifetime for prompt fission neutrons, μs	64.51

3. METHODOLOGY

Diffusion calculations that are made using a diffusion code [16] require macroscopic cross-sections and scattering matrices. They have been generated using the WIMSD-5B code [17]. The Winfrith Improved Multi-group Scheme (WIMS) is a general code for reactor lattice cell calculation on a wide range of reactor systems. In particular, the code will accept rod or plate fuel geometries in either regular arrays or in clusters and the energy group structure has been chosen primarily for calculations.

RSG-GAS is using equilibrium core as a working core, which means by loading pattern 5/1, a stable or constant scheme of fuel refreshing and reshuffling has been derived. After completing the cycle operation, the reactor is in shutdown condition for fuel reshuffling, in order to build the next BOC core configuration. According to the loading pattern 5/1, fuel elements at positions G-8, F-6, D-8, B-8, B-7, and B-5 are taken out as discharged fuel. Then, fuel elements are shifted following the scheme as shown in Table 2. For example, FE at H-9 moves to F-10. Five new FEs and 1 CE are inserted into positions B-9, C-3, C-8, F-3, H-4, and H-9. It is noted that positions B-7, C-8, C-5, D-4, E-9, F-8, F-5, and G-6 are for CE.

Table 2. Fuel element reshuffling at RSG-GAS core by loading pattern 5/1 [6]

From	To	From	To	From	To
H-9	F-10	F-5	F-8	C-7	B-8
H-8	C-4	F-4	F-6	C-6	G-5
H-7	F-7	F-3	C-10	C-5	D-4
H-6	D-10	E-10	B-4	C-4	D-5
H-5	E-5	E-9	G-6	C-3	H-8
H-4	F-9	E-8	D-3	B-9	C-9
G-9	E-8	E-5	A-8	B-8	Out
G-8	Out	E-3	A-7	B-7	Out
G-6	B-7	D-10	G-4	B-5	Out
G-5	G-8	D-8	Out	B-4	A-6
G-4	C-7	D-5	H-5	A-9	A-4
F-10	G-9	D-4	E-9	A-8	B-5
F-9	A-5	D-3	C-6	A-7	H-7
F-8	C-5	C-10	E-3	A-6	B-9
F-7	F-4	C-9	D-8	A-5	H-6
F-6	Out	C-8	F-5	A-4	E-10

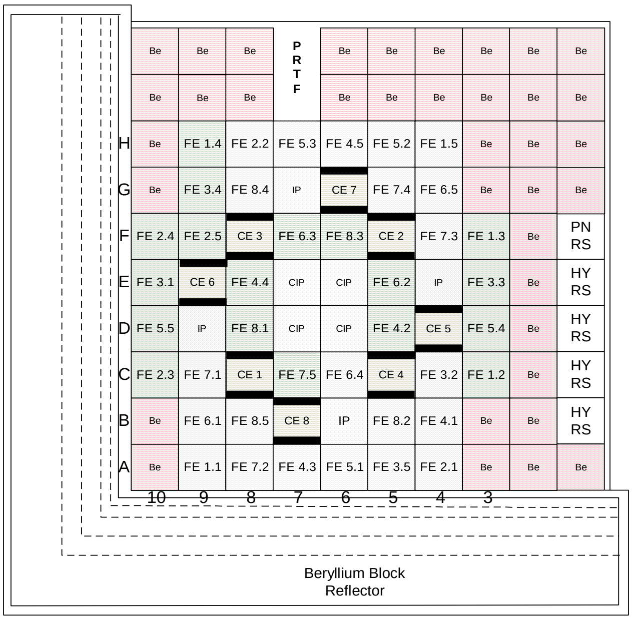

Fig. 1. RSG-GAS core configuration[16]

The basic library has been compiled with 14 fast groups, 13 resonance groups and, 42 thermal groups, but the user is offered the choice of accurate solutions in many groups or rapid calculations in few groups. Temperature-dependent thermal scattering matrices for a variety of scattering laws are included in the library for the principal moderators which include hydrogen, deuterium, graphite, beryllium, and oxygen. The treatment of resonances is based on the use of equivalence theorems with a library of accurately evaluated resonance integrals for equivalent homogeneous systems at a variety of temperatures. The collision theory procedure gives accurate spectrum computations in the 69 groups of the library for the principal regions of the lattice using a simplified geometric representation of complicated lattice cells. The computed spectra are then used for the condensation of cross-sections to the number of groups selected for the solution of the transport equation in detailed geometry. The solution to the transport equation is provided by the use of either the Carlson DSN method or by the collision probability methods. The output of the code provides cell-averaged parameters for use in overall reactor calculations. In this research, macroscopic cross sections for each core zone were calculated based on the PERSEUS method introduced in the slab geometry (plate-type). The WIMSD-5B library file used in this research was produced using the ENDF/B-VII.1 Nuclear Data Bank (NDB). Three partitions of the basic 69-group were selected to homogenize cell data and accommodate integral parameters using FEWGROUPS card. The upper energy group limits were chosen as follows: 10 MeV, 5.531 keV, and 0.625 eV. The radial and axial buckling input to WIMSD-5B are 9.170063E-03 cm^{-2} and 1.764000E-03 cm^{-2}, respectively. They were derived by considering the geometric buckling of a rectangular parallelepiped of 60 cm height and 40.27 cm side length with an 8 cm extrapolation thickness. After generating the group constants for all the reactor components, the group constants were introduced into the Batan-3DIFF code in order to model the reactor core in three dimensions (x-y-z). The fluxes were normalized to 30 MW in the whole core. The axial buckling of 1.709×10^{-3} cm^{2} corresponds to a chopped cosine axial flux distribution with an 8 cm reflector savings. The core calculation (Figure 1) is made of various elements of the reactor core including the SFE, CFE, central irradiation position (central water whole), surrounding water, and beryllium reflector. The Batan-3DIFF code solves the multi-energy-group (up to three) neutron diffusion equation to calculate the effective multiplication factor, power density, and neutron flux distribution in the reactor core. It uses an iterative-based finite difference numerical method on defined control volumes to solve the diffusion equation. Maximum relative changes of the flux and multiplication factor were set to 1.0E-5 and 1.0E-5 respectively for the last iteration as the convergence criteria. The two-dimension and four-group diffusion calculations specified the zone identification of 26 horizontal row regions going from left to right and 24 vertical column regions going from top to bottom.

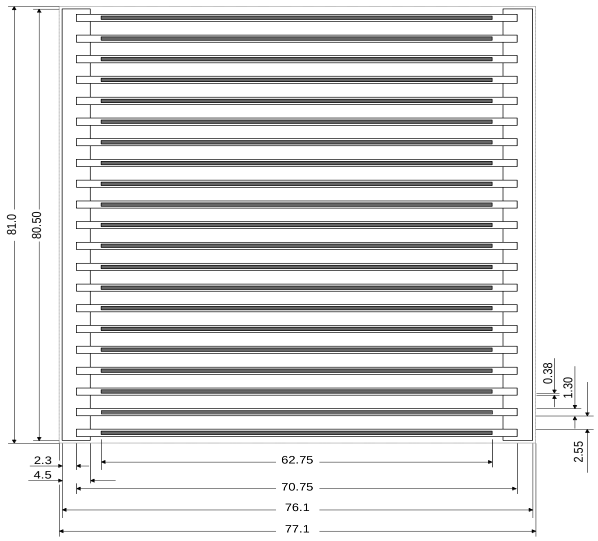

Fig. 2. Standard fuel element of RSG-GAS

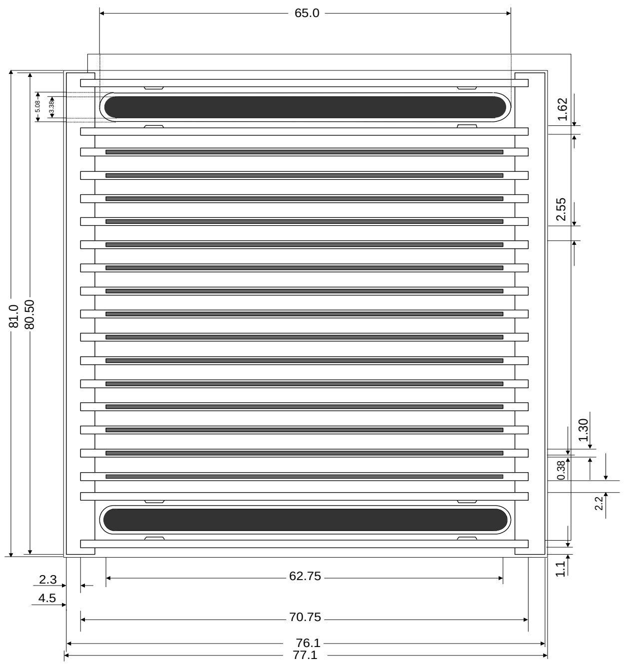

Fig. 3. Control rod fuel element of RSG-GAS

4. RESULTS AND DISCUSSION

Based on the calculated loading pattern, the core is then loaded by fuel element (FE) and control element (CE). The control element is a fuel element containing fork absorber blade as a control rod. Afterward, control rod calibration should be done to get the reactivity worth of the control rods as a function of control rod positions. Control rod calibration of one control rod of the RSG-GAS reactor of core 100 is presented in Figure 4. This S-curve was derived at the critical condition at low power. From the curve, we obtain the control rod worth reactivity, core excess reactivity, and shut down reactivity at 0, 123, 246, 369, 492, and 615 MWD and also PPF values. From the S-curve, it can be seen that at the middle of curve is very sensitive on the neutron in the core for all levels of fuel burnup. It means that it appropriates with the function of control rod for all levels of burnup. These levels of energy release (MWD) represent the burnup. In the case of the RSG-GAS reactor, there are eight control rods. By doing control rod calibration, we can generate a reactivity balance of the reactor core, i.e., the control rod worth reactivity, core excess reactivity, and shutdown reactivity as well as shutdown margin reactivity. The shutdown margin reactivity is derived by subtracting the shut down reactivity by the maximum value of a control rod worth. When the safety conditions, shutdown margin, and core excess reactivity are fulfilled, the reactor can be operated for the cycle operation to serve its utilization.

The methodology of evaluation is by comparing the theoretical fuel management (calculation) and the implementation results of the reactor operation. The comparison covers the main parameter of the cycles operation such as number of fuel loading, reactivity balance, and energy release.

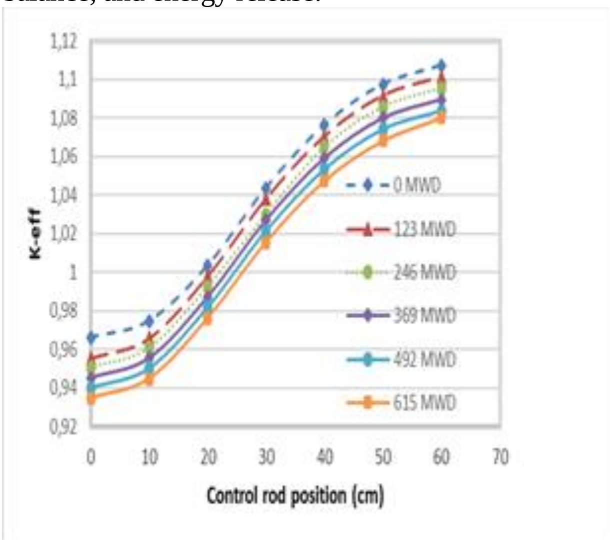

Fig. 4. k_{eff} as a function of burn up and control rod positions

Table 3 presents the results of the PPF values of the RSG-GAS reactor for 0 MWD at the BOC of equilibrium core. The maximum values of radial and axial PPF as a fuction of control rod positions. The value of PPF is not linear with control rod position. Position of control rod at 60 cm means that the total control rods at the bottom of the core. The value of PPF axial and radial is not more the 1.40, which is in accordance to SAR document [15].

Table 3. PPF values of the RSG-GAS for 0 MWD

Control rod position (cm)	Max. Radial PPF	Max. axial PPF	Total PPF	Axial Position
60	1.22	1.30	1.58	D-4
50	1.18	1.40	1.65	D-4
40	1.18	1.56	1.85	D-4
30	1.23	1.74	2.14	D-4
20	1.29	1.82	2.35	D-4
10	1.44	1.45	2.09	E-9
0	1.51	1.29	1.94	H-7

Table 4 show the PPF values of the RSG-GAS reactor core for 123 MWD of burnup. The value of radial PPF is the same with Table 3 axcept at 0 cm control rod position. However, axial PPF value is getting higher at some position of control rod, namely at 0 cm, 10 cm, and 20 cm. It means that there is effect on fuel burnup level on PPF value at RSG-GAS core. There is also an effect to the value of total PPF.

Table 4. PPF values of the RSG-GAS for 123 MWD

Control rod withdrawn (cm)	Max Radial PPF	Max axial PPF	Total PPF	Position in the core
60	1.21	1.30	1.58	D-4
50	1.18	1.40	1.65	D-4
40	1.18	1.56	1.85	D-4
30	1.23	1.74	2.14	D-4
20	1.30	1.82	2.36	D-4
10	1.45	1.45	2.11	E-9
0	1.51	1.28	1.95	H-7

Table 5 show the PPF values of the RSG-GAS core for burnup level of 246 MWD. In this table, the values of axial and radial PPF are still the same at 60 cm control rod position. The of radial PPF change at position of control rod 0 cm, 40 cm, and 50 cm. The change in the value of axial PPF is only at control rod position of 0 cm.

Table 5. PPF values of the RSG-GAS for 246 MWD

Control rod withdrawn (cm)	Max radial PPF	Max axial PPF	Total PPF	Positoin in the core
60	1.22	1.30	1.58	D-4
50	1.17	1.40	1.65	D-4
40	1.19	1.56	1.86	D-4
30	1.23	1.74	2.14	D-4
20	1.29	1.82	2.35	D-4
10	1.44	1.45	2.09	E-9
0	1.50	1.28	1.93	H-7

Table 6 shows the PPF values of the RSG-GAS reactor at 369 MWD. In the table, the values of axial and radial PPF are still the same at the 60 cm control rod position. The values of radial PPF change at the contol rod positions of 0 cm, 10 cm, and 20 cm. For the axial PPF value, change occurs only at the 30 cm control rod position.

Table 6. PPF values of the RSG-GAS for 369 MWD

Control rod withdrawn (cm)	Max radial PPF	Max axial PPF	Total PPF	Position in the core
60	1.22	1.30	1.58	D-4
50	1.18	1.40	1.65	D-4
40	1.18	1.56	1.85	D-4
30	1.23	1.75	1.15	D-4
20	1.31	1.82	2.37	D-4
10	1.46	1.45	2.11	E-9
0	1.52	1.29	1.96	H-7

Table 7 shows the PPF values of the RSG-GAS reactor at 492 MWD burnup level. In this table, the values of axial and radial PPF are still the same at 60 cm control rod position. The value of radial PPF changes only at contol rod position of 0 cm, similar with what occurs in axial PPF.

Table 7. PPF values of the RSG-GAS for 492 MWD

Control rod withdrawn (cm	Max radial PPF	Max axial PPF	Total PPF	Position in the core
60	1.22	1.30	1.58	D-4
50	1.18	1.40	1.65	D-4
40	1.18	1.56	1.85	D-4
30	1.23	1.74	2.14	D-4
20	1.29	1.82	2.35	D-4
10	1.44	1.45	2.09	E-9
0	1.50	1.28	1.93	H-7

Table 8 shows the PPF values of the RSG-GAS core at 615 MWD, the EOC of equilibrium core. The values of radial PPF change only at all positions apart from 50 cm control rod position, whom has the same value as the reference. The values of axial PPF are higher than the value of radial PPF reference (0 MWD) change. Only at contol rod position of 0 cm the value is the same with reference.

Table 8. PPF values of the RSG-GAS for 615 MWD

Control rod withdrawn (cm)	Max radial PPF	Max axial PPF	Total PPF	Position in the core
60	1.17	1.40	1.65	D-4
50	1.18	1.50	1.78	D-4
40	1.20	1.56	1.87	D-4
30	1.24	1.75	2.17	D-4
20	1.32	1.83	2.42	D-4
10	1.48	1.45	2.14	E-9
0	1.54	1.29	1.99	H-7

5. CONCLUSION

From the result of calculation, it can be concluded that the values of axial and radial PPF always depend on fuel burnup and position of control rods. The values of axial and radial PPF are still below the safety limit. The results supports the conduct of operation in a safe manner for optimal utilization with stable parameters and under stable safety conditions. The core excess reactivity, shutdown margin, control rod worth, and PPF of different burnup was performed using a verified three-dimensional, four-group diffusion calculation code.

ACKNOWLEDGMENT

This work is supported by DIPA budget of 2021. The authors wish to thank the Head of PRTRN-ORTN, BRIN and the coordinator of BFTR-PRTRN for their kindly help and useful discussions when doing the research.

AUTHOR CONTRIBUTION

Lily Suparlina carried out core modelling in core calculation code, Purwadi carried out cell calculation using WIMSD-5B. Kunihito Nabeshima participated as a reviewer and data analysis, Lily Suparlina, Purwadi, and Kunihito Nabeshima are the main contributors of this paper. All authors read and approved the final version of the manuscript.

REFERENCES

1. Pinem S., Sembiring T.M., Surbakti T. Core Conversion Design Study of TRIGA Mark 2000 Bandung using MTR Plate Type Fuel Element. Int. J. Nucl. Energy Sci. Technol. 2018. **12**(3):222-238.
2. Surbakti T., Purwadi P. Analysis of Neutronic Safety Parameters of the Multi-Purpose Reactor–Gerrit Augustinus Siwabessy (RSG-GAS) Research Reactor at Serpong. J. Penelit. Fis. dan Apl. 2019. **9**(1):78-91.
3. Liem P.H., Surbakti T., Hartanto D. Kinetics Parameters Evaluation on the First Core of the RSG GAS (MPR-30) using Continuous Energy Monte Carlo Method. Prog. Nucl. Energy. 2018. **109**(June):196–203.
4. Dawahra S., Khattab K., Saba G. Extending the Maximum Operation Time of the MNSR Reactor. Appl. Radiat. Isot. 2016. **115**:256-261.
5. Dawahra S., Khattab K., Saba G. Calculation and Comparison of Xenon and Samarium Reactivities of the HEU, LEU Core in the Low Power Research Reactor. Appl. Radiat. Isot. 2015. **101**:27–32.
6. Surbakti T., Pinem S., Suparlina L. Dynamic Analysis on the Safety Criteria of the Conceptual Core Design in MTR-type Research Reactor. Atom Indonesia. 2018. **44**(2):89-97.
7. Surbakti T., Pinem S., Sembiring T.M., Hamzah A., Nabeshima K. Calculation of Control Rods Reactivity Worth of RSG-GAS First Core using Deterministic and Monte Carlo Methods. Atom Indones. 2019. **45**(2):69–79.
8. Pinem S., Sembiring T.M., Liem P.H. Neutronic and Thermal-hydraulic Safety Analysis for the Optimization of the Uranium Foil Target in the RSG-GAS Reactor. Atom Indonesia. 2016. **42**(3):123–128.
9. Surbakti T., Pinem S., Sembiring T.M., Subekti M., Sunaryo G.R. Preliminary Study for Alternative Conceptual Core Design of the MTR Research Reactor. J. Phys. Conf. Ser. 2018. **962**(1)
10. Hedayat A. Benchmarking Verification of the Control Rod Effects on the MTR Core Parameters using the MTR-PC and MCNP Codes throughout 3D Core Modeling and Rod-drop Experiment. Prog. Nucl. Energy. 2016. **88**:183-190.
11. Liu Z., Smith K., Forget B. Calculation of Multi-group Migration Areas in Deterministic Transport Simulations. Ann. Nucl. Energy. 2020. **140**:107-110.
12. Wang C., Liu L., Liu M., Zhang D., Tian W., Qiu S., et al. Conceptual Design and Analysis of Heat Pipe Cooled Silo Cooling System for the Transportable Fluoride-salt-cooled High-temperature Reactor. Ann. Nucl. Energy. 2017. **109**
13. Pinem S., Liem P.H., Sembiring T.M.,

Surbakti T. Fuel Element Burnup Measurements for the Equilibrium LEU Silicide RSG GAS (MPR-30) Core under a New Fuel Management Strategy. Ann. Nucl. Energy. 2016. **98**

14. Villarino E.A., Mochi I. Thermal-hydraulic Models for Neutronic and thermaly- hydraulic Feedback in Citvap Code. 2014. **23**:23-36.
15. Surbakti T., Imron M. Fuel Burn-up Calculation for Working Core of the RSG-GAS Research Reactor at Batan Serpong. J. Penelit. Fis. dan Apl. 2017. **7**(2):89-101.
16. Pinem S., Surbakti T., Sembiring T. Optimization of Radioisotope Production at RSG-GAS Reactor using Deterministic Method. Journal Teknologi Indonesia 2016. 1 (2):12-18.
17. Valtavirta V., Leppänen J., Viitanen T. Coupled Neutronics–fuel Behavior Calculations in Steady State using the Serpent 2 Monte Carlo Code. Ann. Nucl. Energy. 2017. **100**